

Article

Utilization of Thermally Activated Building System with Horizontal Ground Heat Exchanger Considering the Weather Conditions

Woong June Chung ¹  and Sang Hoon Park ^{2,*} 

¹ Department of Equipment and Fire Protection Engineering, College of Engineering, Gachon University, Seongnam 13120, Korea; wjchung@gachon.ac.kr

² Division of Architecture, College of Engineering, Sun Moon University, Asan 31460, Korea

* Correspondence: sanghoon@sunmoon.ac.kr

Abstract: The thermally activated building system (TABS) can reduce the peak load by integrating with the ground heat exchangers. When integrated, the cost of groundwork and stability of the ground temperature would counteract because the weather conditions would influence the ground temperature in shallow depth. However, previous studies on TABS assumed constant ground temperatures such as average outdoor air temperature. In this study, ground temperatures in different depths are simulated for their detailed investigations, and simulated results of ground temperature were applied to building energy simulations for observing the load-handled ratio (LHR), representing the peak load reduction by TABS evaluated in various weather conditions. Simulation results of ground temperatures from 1 m to 39 m depths show that the temperature stabilized at 2 m to 11 m depths depending on the characteristics of the outdoor air temperature. LHR increased as the ground depth increased because the ground temperature at shallow depths increased during peak hours. Ground depths of 8 m were found ideal for maintaining consistent LHR for all weather conditions. Detailed observation of ground temperature and its effect on LHR in various weather conditions can help system engineers design and operate the TABS with the ground system.

Keywords: thermally activated building system; ground heat exchanger; load-handled ratio; EnergyPlus; KIVA



Citation: Chung, W.J.; Park, S.H. Utilization of Thermally Activated Building System with Horizontal Ground Heat Exchanger Considering the Weather Conditions. *Energies* **2021**, *14*, 7927. <https://doi.org/10.3390/en14237927>

Academic Editor:
Alessandro Cannavale

Received: 22 October 2021
Accepted: 23 November 2021
Published: 26 November 2021

Publisher's Note: MDPI stays neutral with regard to jurisdictional claims in published maps and institutional affiliations.



Copyright: © 2021 by the authors. Licensee MDPI, Basel, Switzerland. This article is an open access article distributed under the terms and conditions of the Creative Commons Attribution (CC BY) license (<https://creativecommons.org/licenses/by/4.0/>).

1. Introduction

The climate change from global warming, energy consumption to maintain an optimal indoor environment, and urbanization have increased the peak building load. The demand for more reserve power from the power plant for stable operation may lead to electricity wastage [1]. Building energy use is responsible for a significant portion of energy consumption among the transportation, industrial, and building sectors, with the main contributor being the cooling load. Previous research on reducing the peak cooling load of the building was based on passive and active technologies. The passive technologies are related to the building fabric, such as building thermal mass, phase-change-material, green roof, and cool roof [2–5]. The active technologies are related to the system, such as storage tanks, thermally activated building systems (TABS), and pre-cooling strategies [1,6,7].

Among many peak reduction technologies, TABS actively uses the building concrete structure having a relatively large heat capacity. Peak load can be reduced due to the asynchrony of heavy structures, which store the heat during non-demand periods for use during peak periods [8,9]. During the cooling period, TABS is designed to be placed on the ceiling, roof, and wall of the controlled zone, having a large exposed surface for heat exchange between the zone and system. The basic control of TABS is based on the self-regulation effect, which uses supply water temperature close to the zone setpoint temperature and removes the load depending on the temperature difference between the zone and TABS surface [10–13]. Higher cooling and lower heating supply water

temperature of TABS makes it easier to apply renewable energy sources such as geothermal systems. Because the underground temperature is relatively constant, a simple heat exchanger may lead to free cooling without a heat pump [14–16]. In previous studies, TABS integrated with a ground heat exchanger is evaluated for limited condition. However, the evaluation of its effectiveness in various weather conditions is yet to be found.

In the design stage, the ground temperatures are often assumed as constant [17], in which case, the supply water temperature of TABS is assumed to be consistent. However, the ground temperature varies depending on the weather conditions and ground depth, especially for the horizontal ground system, which will impact the effectiveness of TABS [18,19]. In this study, the ground temperatures according to the weather conditions at different depths are assessed with detailed ground simulations. The effectiveness of TABS on reducing the peak cooling load is then evaluated with building energy simulations by comparing the amount of the cooling load handled by TABS. The overall research process of the detailed evaluations is demonstrated in Figure 1.

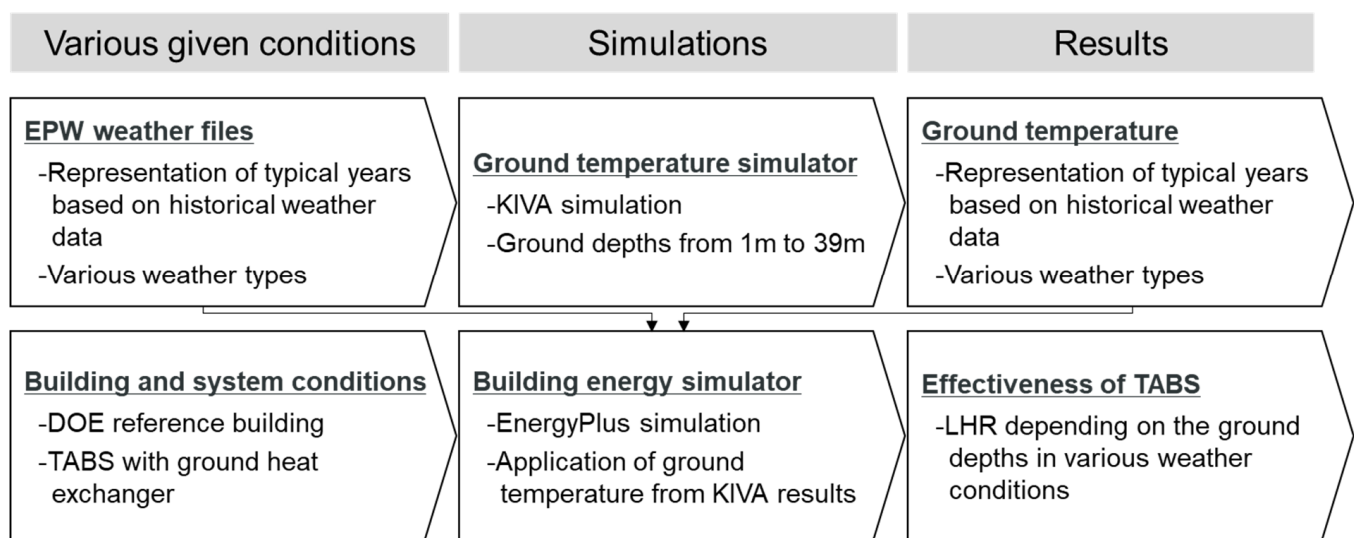


Figure 1. Flow chart of the study on evaluation of TABS integrated with ground exchanger.

2. Analysis of Ground Temperature in Various Conditions

2.1. Selection of Weather Locations

Ground temperature is commonly considered to be consistent because of the high heat capacity characteristics of the ground. As the weather is one of the primary factors influencing the ground temperature, the average outdoor air temperature is assumed to be equivalent to the ground temperature deep underground. However, the weather conditions change throughout the year, and the impact varies depending on the depth. Thus, the weather conditions and depth of the heat exchanger should be considered while designing geothermal systems. More importantly, TABS integrated with horizontal ground heat exchanger must consider the ground temperature because the supply water temperature depends on the ground temperature. Therefore, the ground temperatures in various weather conditions should be calculated to evaluate the performance of TABS integrated with a horizontal ground heat exchanger.

We use the conventional Köppen–Geiger climate classification system [20–24] to observe the ground temperature in various weather conditions. The system divides the weather into five main groups, namely equatorial (A), arid (B), warm temperate (C), snow (D), and polar (E). The weather is further distinguished based on precipitation and temperature, as desert (W), steppe (S), fully humid (f), summer dry (s), winter dry (w), monsoonal (m), hot arid (h), cold arid (k), hot summer (a), warm summer (b), cool summer (c), extremely continental (d), frost (F), and tundra (T). From the 31 Köppen–Geiger climate classifications, 28 weather files were selected by visual observation from the Köppen–Geiger

climate classification map. Cwc, Dsd, and EF climate classifications were excluded from the study because weather stations were not located in those areas. The country and city information of weather based on the weather files from the energyplus website [25] are listed in Table 1.

Table 1. Weather selection with Koppen–Geiger climate classification.

Main Climate Classification	Koppen-Geiger Class	Koppen–Geiger Sub-Climate Type	Country	City
Equatorial	Af	Fully humid	Malaysia	Kuching
	Am	Monsoonal	Philippines	Manila
	As	Summer dry	India	Indore
	Aw	Winter dry	Thailand	Bangkok
Arid	BSh	Steppe hot	Kenya	Garissa
	BSk	Steppe cold	China	Beijing
	BWh	Desert hot	Egypt	Kharga
	BWk	Desert cold	China	Kuqa
Warm Temperate	Cfa	Fully humid hot summer	Argentina	Buenos Aires
	Cfb	Fully humid warm summer	Colombia	Bogota
	Cfc	Fully humid cool summer	Iceland	Reykjavik
	Csa	Summer dry hot summer	Morocco	Casablanca
	Csb	Summer dry warm summer	South Africa	Cape Town
	Csc	Summer dry cool summer	United States	Kahului
	Cwa	Winter dry hot summer	India	New Delhi
	Cwb	Winter dry warm summer	Peru	Cusco
	Cwc	Winter dry cool summer	lack of pixel and no weather file	
Snow	Dfa	Fully humid hot summer	Korea	Kangnung
	Dfb	Fully humid warm summer	Japan	Sapporo
	Dfc	Fully humid cool summer	United States	Anchorage
	Dfd	Fully humid extremely continental	Russia	Yakutsk
	Dsa	Summer dry hot summer	United States	Ogden-Hill
	Dsb	Summer dry warm summer	United States	Flagstaff-Pulliam
	Dsc	Summer dry cool summer	United States	Homer
	Dsd	Summer dry extremely continental	No weather file	
	Dwa	Winter dry hot summer	China	Harbin
	Dwb	Winter dry warm summer	Russia	Irkutsk
	Dwc	Winter dry cool summer	China	Xinghai
	Dwd	Winter dry extremely continental	China	Qumarleb
Polar	EF	Polar frost	No weather file	
	ET	Polar tundra	China	Tibet

The outdoor air temperature and humidity ratio of each weather location are plotted in Figure 2. Across weather locations, the outdoor air temperature ranged from -48.3 °C to 47.3 °C and humidity ratio from 0.00001 to 0.027. The minimum and maximum variation of outdoor air temperature in a single weather location was 13 °C in Af (Kuching) and 80 °C in Dfd (Yakutsk), respectively. When the weather condition has a high humidity ratio, the outdoor temperature has a small variation, and vice-versa, because the humidity in the air works as the heat storage, limiting the variations in the outdoor air temperature. The large variations in the outdoor air temperature and humidity ratio of the selected weather conditions may cover most weather conditions, which is sufficient to evaluate the ground temperatures in various situations.

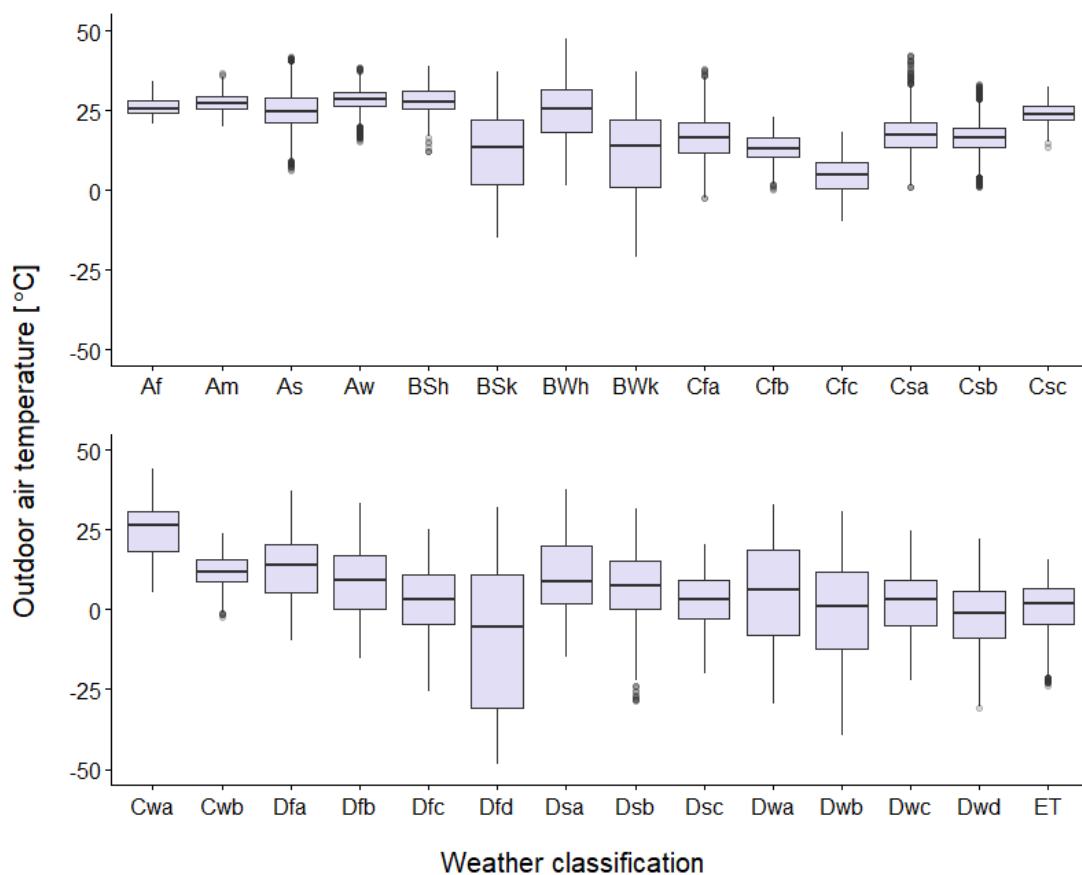
2.2. Analysis of Ground Temperature and Parameters to Consider in TABS

The ground temperatures should be calculated with a simulation tool for precision and accuracy. One of the sophisticated ground heat transfer calculation tools, KIVA v0.5.0, was used to calculate the hourly ground temperature throughout the year. The tool uses a two-dimensional finite difference method to calculate the temperature at different

depths and study the impact of weather conditions [26]. As the deep ground depth in the simulation tool was set to 40 m, the ground temperatures at 1 m to 39 m depths were calculated at increments of 1 m for the 28 weather conditions. Since the typical horizontal ground system is 0.5 m to 3 m depth, the depth of 39 m will be sufficient to cover most of the weather conditions [18,27]. A total of 812 simulations covering the different weather conditions were conducted using MATLAB R2021a.

Two factors to consider when operating the TABS integrated with a horizontal ground heat exchanger are the ground temperatures below the water freezing point and variations in ground temperature. For ground temperatures below the freezing point, the risk of damaging the pipes and system would increase. The median ground temperature at eight weather locations, Dfc (Anchorage), Dfd (Yakutsk), Dsc (Homer), Dwa (Harbin), Dwb (Irkutsk), Dwc (Xinghai), Dwd (Qumarleb), and ET (Tibet), demonstrated below freezing point temperatures (Figure 3). These locations may have a high risk of coolant freezing.

The variations in ground temperature may impact the peak reduction achieved by the TABS. For observing the ground temperature variation due to the weather conditions, the ground temperatures at the shallowest depth from the previous study, 0.5 m, are presented in Figure 3. The minimum and maximum variation in ground temperatures is 2.9 °C in Kahului and 13.1 °C in Yakutsk, respectively. Although the location with the minimum variation in ground temperature did not coincide with that having minimum variation in outdoor air temperature, the trend was similar. The difference in outdoor air and ground temperature may deviate because other weather factors, such as solar radiation and wind speed, were used in calculating the ground temperature.



(a)

Figure 2. Cont.

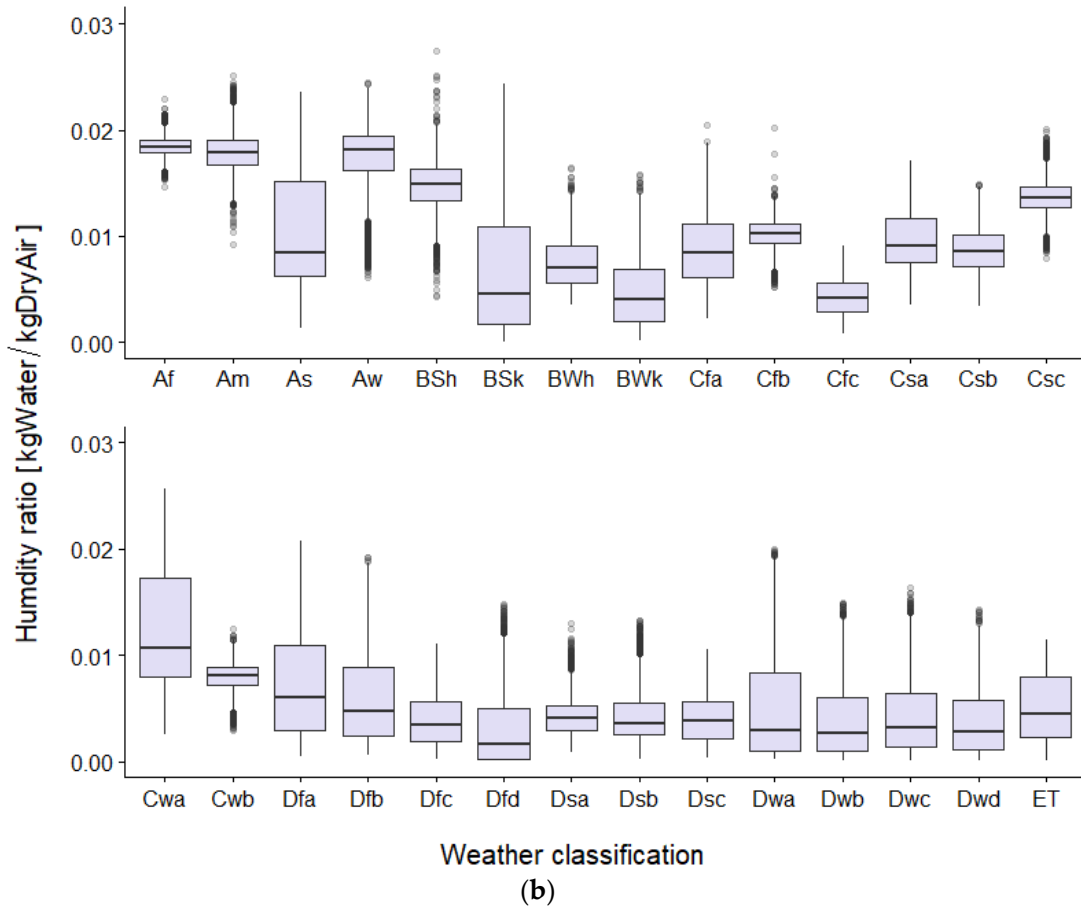


Figure 2. Weather conditions according to Koppen–Geiger climate classification: (a) outdoor air temperature; (b) humidity ratio.

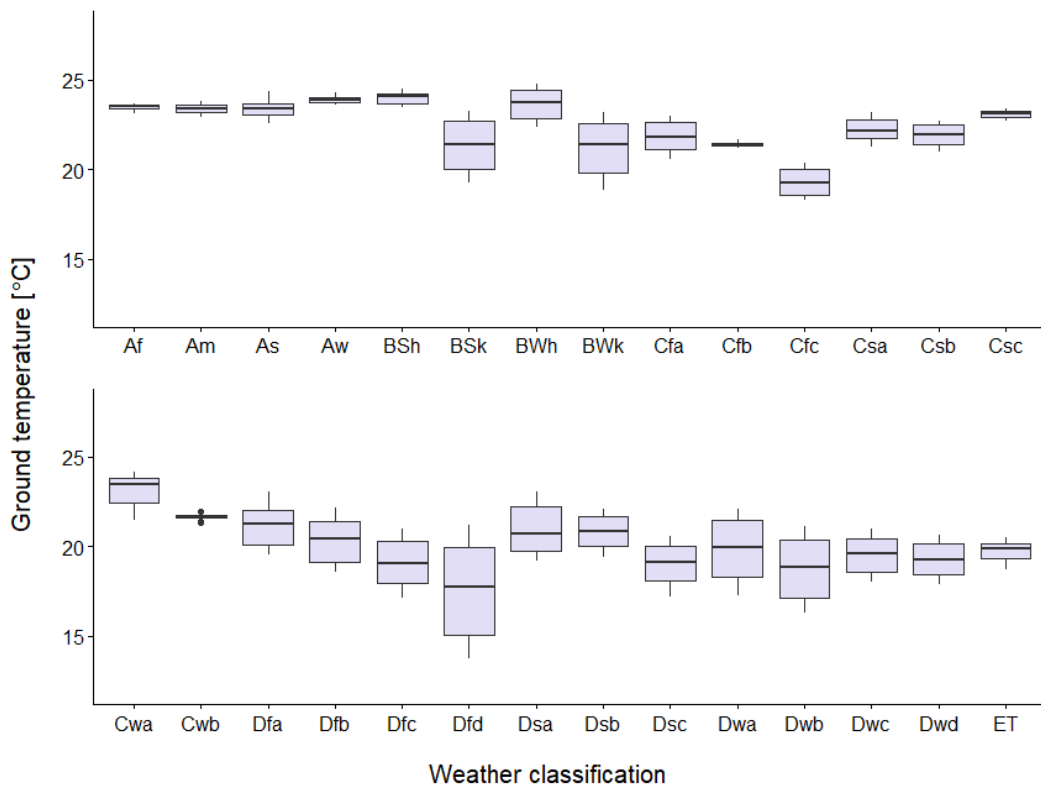


Figure 3. Shallow ground temperature comparison among different weather conditions.

Because the 0.5 m shallow depth demonstrated significantly large variations in ground temperatures, the weather conditions from the five main climate classifications were selected for its detailed observations. Within the main climate classification, the weather with a relatively large difference between the minimum and maximum value of ground temperature was selected, namely As (Indore), BSk (Beijing), Cfa (Buenos Aires), Dfd (Yakutsk), and ET (Tibet). These regions also had a relatively low humidity ratio compared to other locations within the main climate classification. The ranges in ground temperature in depths of 1 m to 39 m are presented in Figure 4. For shallow depths, the ground temperature varies significantly. The variation reduces with increasing ground depth because the deep ground temperature was relatively consistent. The previous study had a similar result and indicated that the BSk (Tabriz) had approximately 11 degrees Celsius for deep ground temperature and demonstrated stability in 8 m to 10 m depth [28]. In Figure 5, the variations in ground temperatures at different depths are plotted. We conclude that the ground depth has to be maintained at 11 m for a consistent ground temperature difference of 2 °C at all times. However, in humid weather conditions, the ground depth can be as low as 2 m to achieve consistent ground temperature.

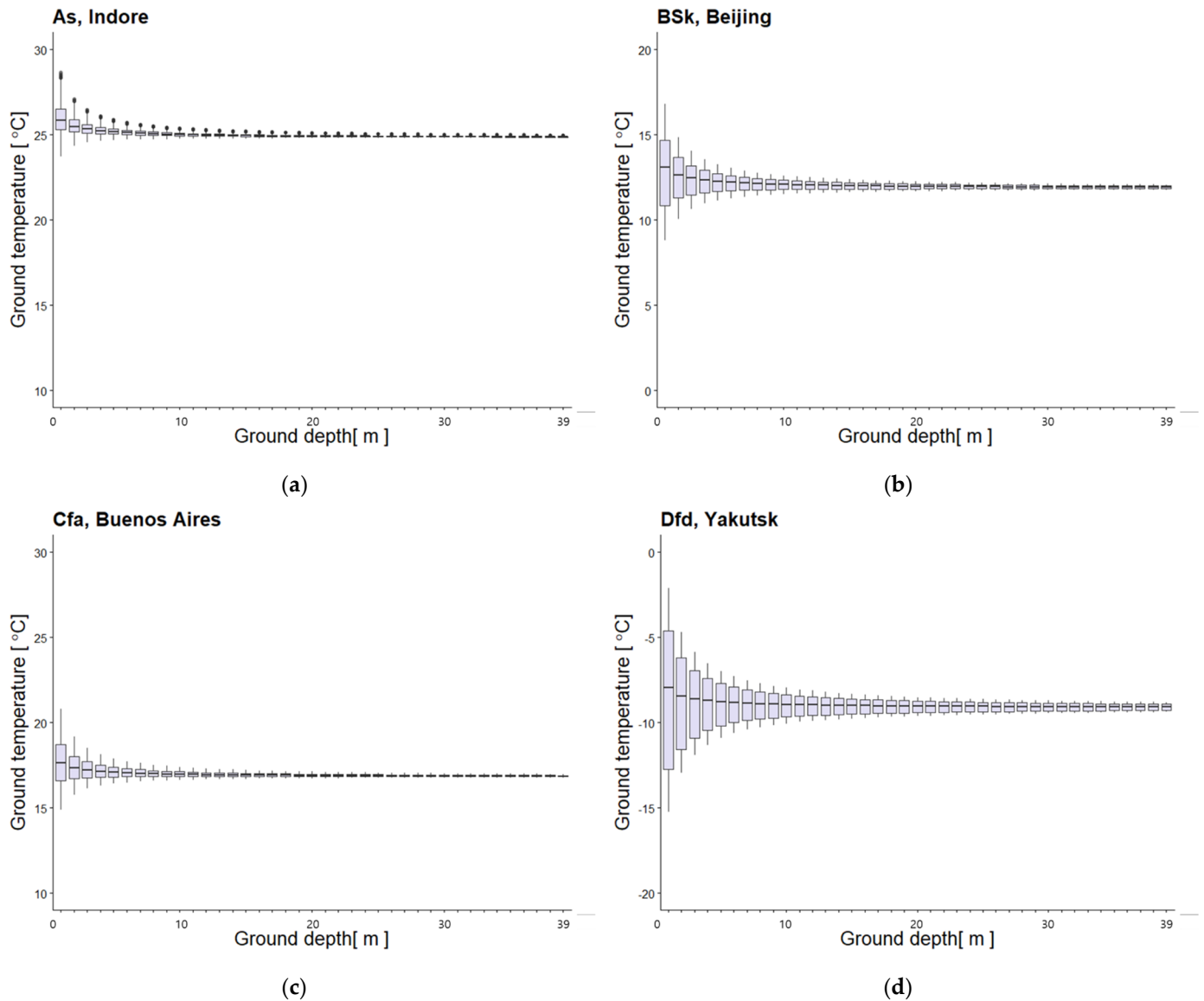
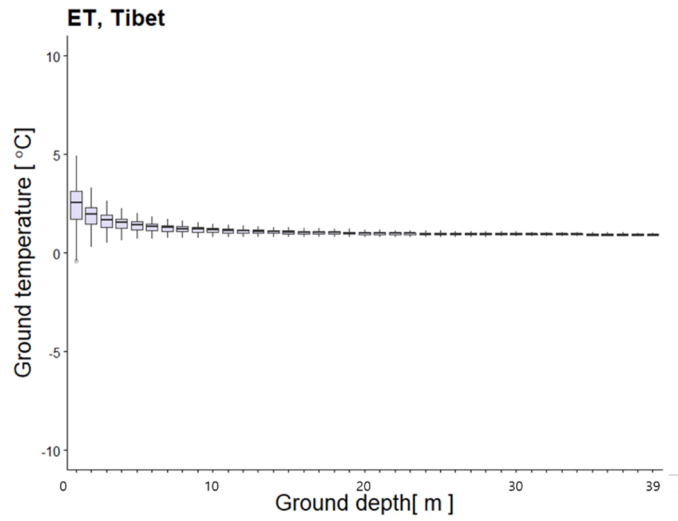


Figure 4. Cont.



(e)

Figure 4. Ground temperatures at different depth: (a) as, Indore; (b) BSk, Beijing; (c) Cfa, Buenos Aires; (d) Dfd, Yaktsk; (e) ET, Tibet.

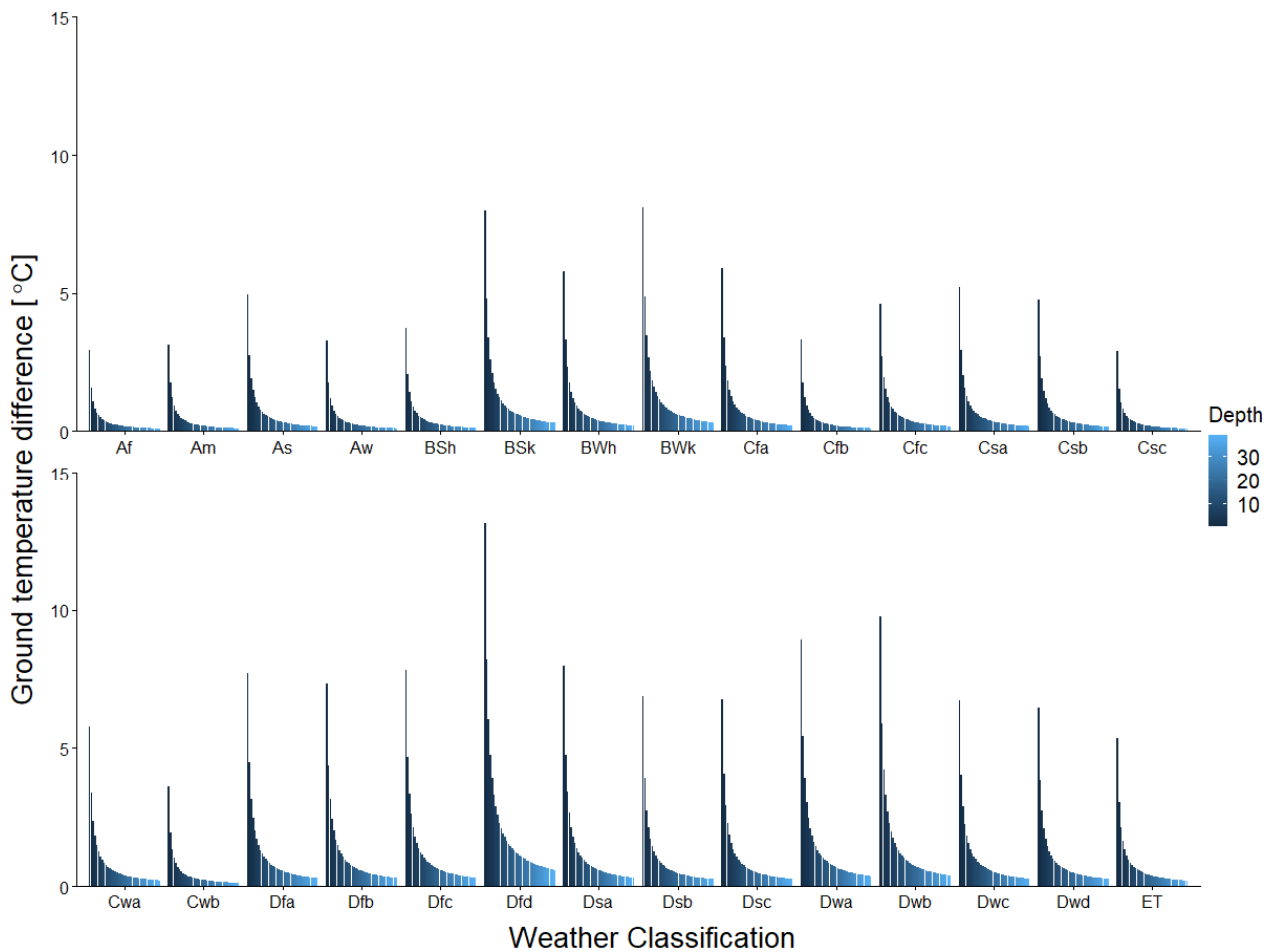


Figure 5. Ground temperature depending on weather and ground depth.

3. Results and Discussions

3.1. Simulation Setup and Load-Handled Ratio of TABS

Specification of building materials and size of reference building from the Department of Energy (DOE) was used for representing a typical small office building. DOE proposes 16 reference building types covering most commercial buildings across the 16 different locations. The new construction reference building condition from a temperate weather location, Chicago, was used in this study. The office occupancy schedule proposed by DOE was used [29]. The overview of the small single-story office building with attic space and window to wall ratio of approximately 21% is shown in Figure 6. For analyzing the building load, EnergyPlus version 9.4 was used to model the building and system. EnergyPlus is commercial software that was validated through various experiments [30–32]. Boundary conditions used for simulations are given in Table 2.

The schematic of TABS integrated with a horizontal ground heat exchanger is shown in Figure 7. The pipes of TABS are directly connected to the ground system and have a heat exchanger between the systems. The TABS is placed on the ceiling of the conditioned zone for improving thermal comfort because one of the local thermal discomfort, the vertical air temperature difference between the feet and head, needs to be maintained within approximately three degrees [33]. The ground temperatures from KIVA simulation results were used. As the EnergyPlus simulation requires hourly ground temperature and only allows the average soil temperature and average ground temperature as input values, the average, and range obtained from KIVA were used. Although the ground temperature may change depending on the system used and require a recovery period, consistent ground temperatures were assumed for evaluating the maximum potential of the TABS in this study.

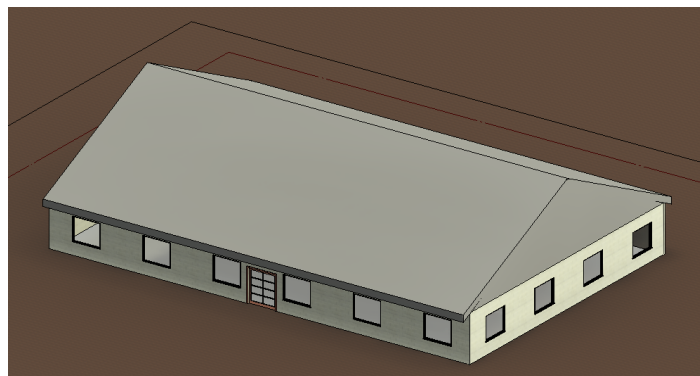


Figure 6. Overview of a small office building from DOE reference building.

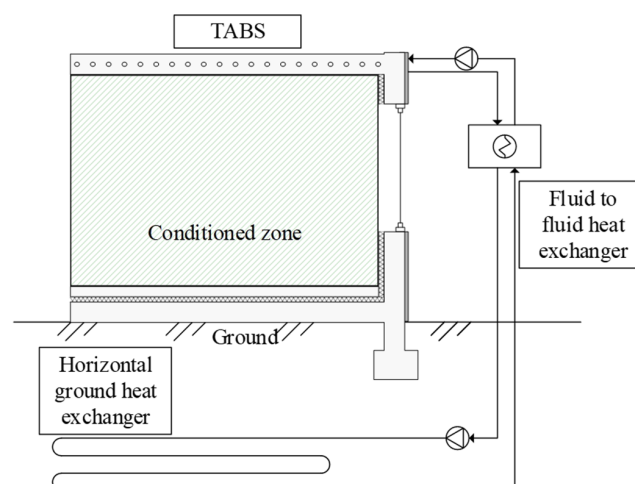


Figure 7. Schematic of TABS integrated with horizontal ground heat exchanger.

Table 2. Boundary conditions used in the simulations.

Conditions	Contents
Zone area	511 m ² (27.69 m × 18.46 m)
U-value of the wall	0.698 W/m ² K
SHGC and U-value of windows	0.391, 3.241 W/m ² K
Wall construction	0.025 m Stucco, 0.203 m concrete, 0.066 m insulation, 0.013 m gypsum board
Ceiling construction	0.146 m insulation, 0.203 m concrete, 0.013 m gypsum board
Internal heat gain	People: 18.58 m ² /person Lighting: 10.76 W/m ² Equipment: 10.76 W/m ²
Setpoint temperature	24 °C (summer)
Infiltration rate	0.34 ACH
Occupancy schedule	Office working hours (weekdays from 09:00 to 18:00)

As TABS actively uses the building thermal mass by embedding pipes into the concrete structure, the system stores the heat into the heavy mass during the non-peak period for use during the peak hour, as described in Figure 8. Therefore, the efficiency of TABS is evaluated by calculating the ratio of load handled by TABS and maximum load during the peak hour as follows [34]:

$$LHR_{cooling} = \frac{q_{TABS,cooling}}{q_{max,cooling}} \times 100\% \quad (1)$$

Because the weather conditions vary significantly, the typical load-handled ratio (LHR) of TABS would be different for each weather condition. The TABS with supply water temperature of 24 °C, which is the zone setpoint temperature, was simulated to observe the typical LHR of TABS in various weather conditions. The simulation results are demonstrated in Figure 9. LHR of TABS is low or zero when the outdoor air temperature is relatively low, such as during summers, because the cooling load from solar radiation and internal heat gain are lower than the heat loss from infiltration and external façade. The average LHR is 18.4%, and the highest is 32.4% in BSh (Garissa).

3.2. Load Handled Ratio According to Ground System Depth

In simulations, fluids had below freezing point temperature for all ground depths in Cfc (Reykjavik), Dfc (Anchorage), Dfd (Yakutsk), Dwa (Harbin), Dwb (Irkutsk), Dwc (Xinghai), Dwd (Qumarleb), and ET (Tibet). The locations with the median ground temperature below the freezing point temperature in the previous section were similar in the simulation results. However, a couple of weather locations experienced varying results. Cfc (Reykjavik), where the median ground temperature was 1.4 °C, had system fluid below freezing point temperature, whereas Dcs (Homer) that had −2.4 °C of median ground temperature could maintain above freezing point temperature. Therefore, the hourly ground temperature is significant when assessing the ground system feasibility.

As TABS is a radiant cooling system, the condensation risk is an important factor to consider, as it may cause mold and damage the surface materials. Excluding the weather locations with fluids below freezing point temperature, the condensation occurred in BSk (Beijing), Dfa (Kangnung), and Dfb (Sapporo). The hours of condensation risk depending on the weather and ground depths are illustrated in Figure 10. Three weather locations had a high humidity ratio and wide range and amplitude of outdoor air temperature compared to other weather conditions. Because the shallow ground depth has a higher ground temperature during the summer period, the supply water temperature decreased as the ground depth increased. During the spring and autumn periods, the supply water temperature may increase while ground depth increases. However, the summer may experience indoor condensation and not influence the number of hours of condensation. Hence, the hours of condensation increase as the ground system depth increases in all cases.

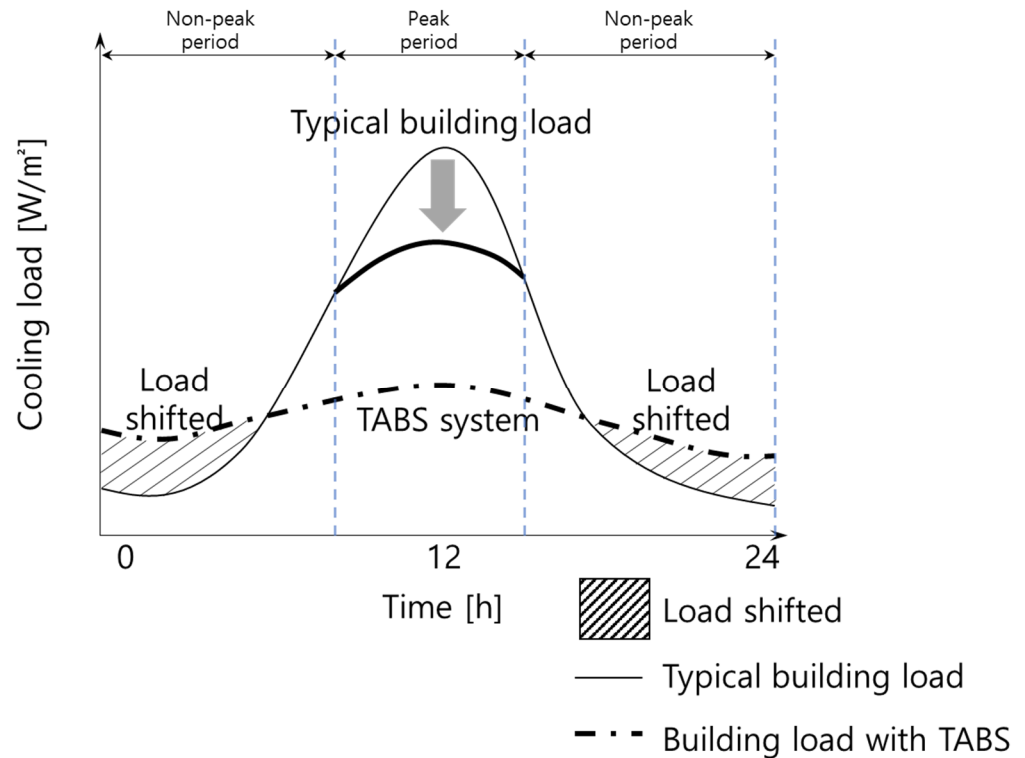


Figure 8. Concept of peak reduction by TABS.

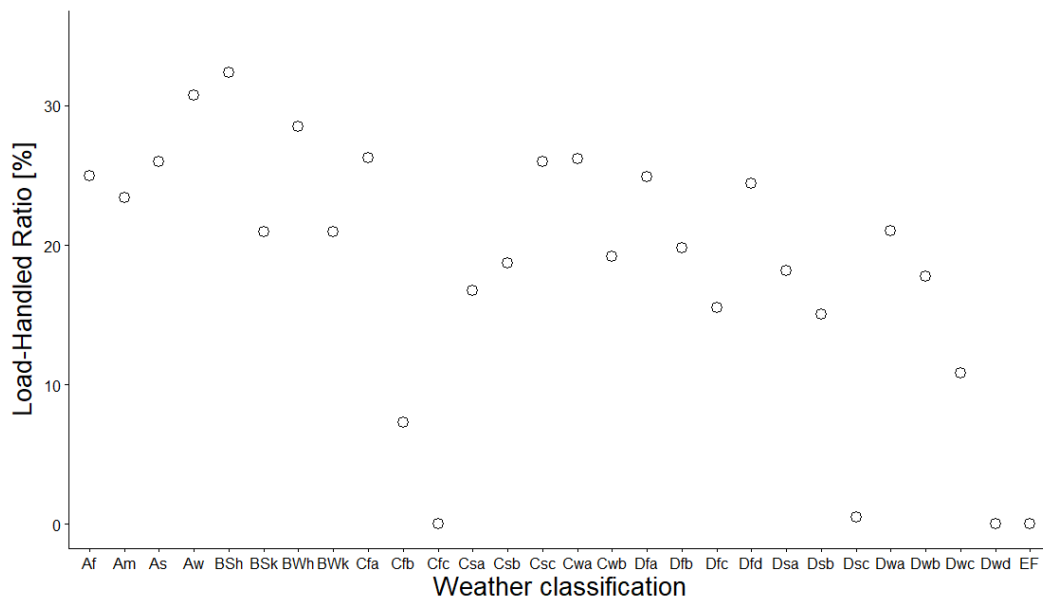


Figure 9. LHR with typical self-regulation strategy.

The LHR of TABS, depending on the ground depth and typical LHR in weather locations excluding the condensation and frozen fluid, are presented in Figure 11. Basic TABS control strategies with self-regulation effectively reduced the peak load in relatively hot and dry weather conditions. However, the supply water directly connected to the heat exchanger also had a high temperature in hot regions. Thus, four weather locations, Af (Kuching), Am (Manila), Aw (Bangkok), and BSh (Garissa), could not achieve free cooling. In contrast, Cfb (Bogota) was expected to have a low peak reduction in the typical control strategy while it achieved 66% LHR. The maximum possible LHR was 75% in Dsb (Flagstaff-Pulliam), while the typical strategy could only reduce 32.4% in BSh (Garissa).

More detailed LHR changes depending on the ground depth are illustrated in Figure 12. The LHR increases as the ground depth increase because the shallow ground temperatures are higher than the deep ground temperature during the peak period, with a maximum difference of 11% in BWh (Kharga). However, as the ground temperature stabilizes, the LHR difference is reduced to 1% after 8 m of ground depth, which is considered an adequate ground depth design for maintaining a stable LHR for TABS. In previous studies, Dwa (Seoul) was recommended to have 40% to 50% of LHR with the ground heat pump system. The results indicated that the ground heat exchanger had a higher potential to reduce the peak load with the ground heat exchanger [17,34].

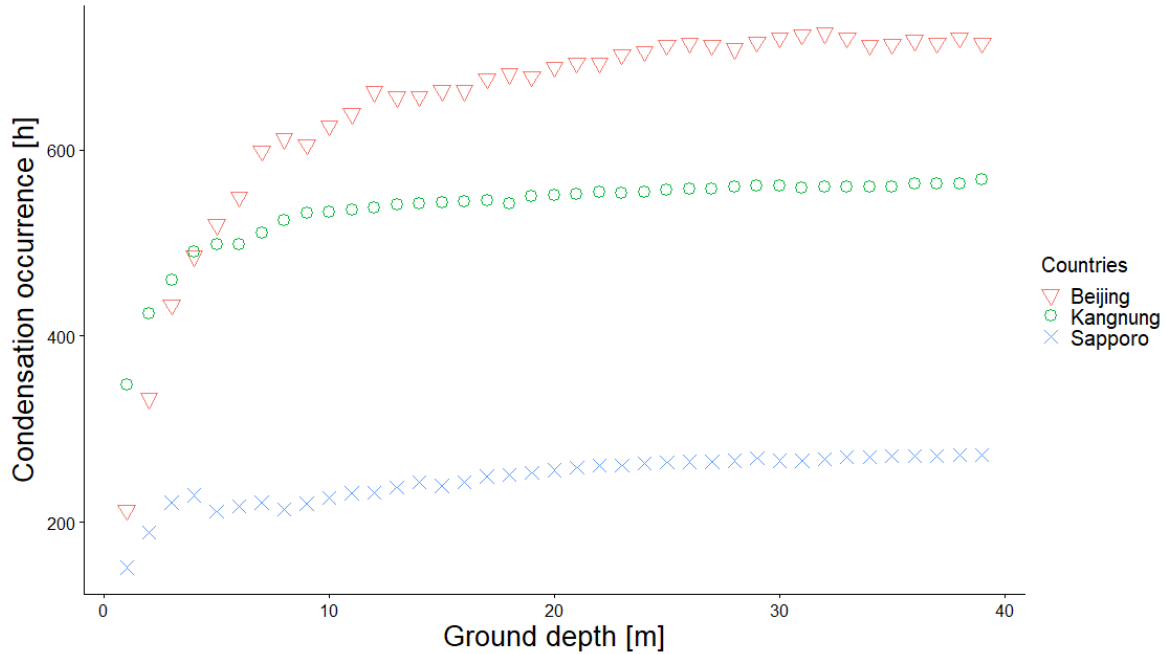


Figure 10. Hours of condensation risk in BSk (Beijing), Dfa (Kangnung), and Dfb (Sapporo).

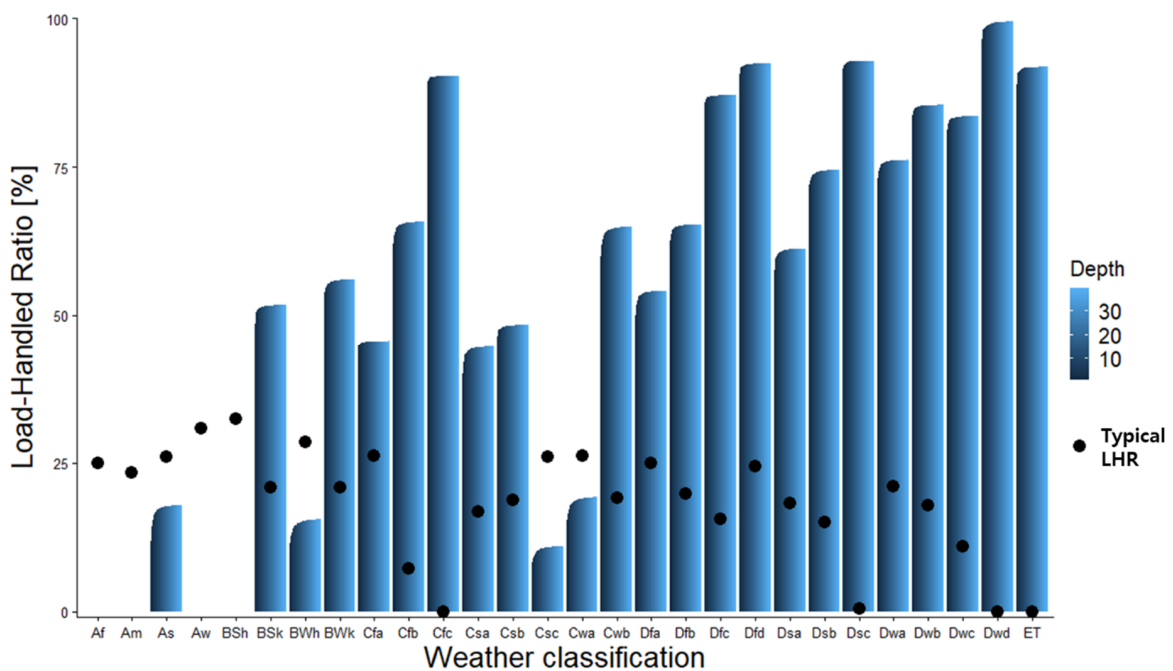


Figure 11. Comparison of typical LHR and application of ground calculation in simulation.

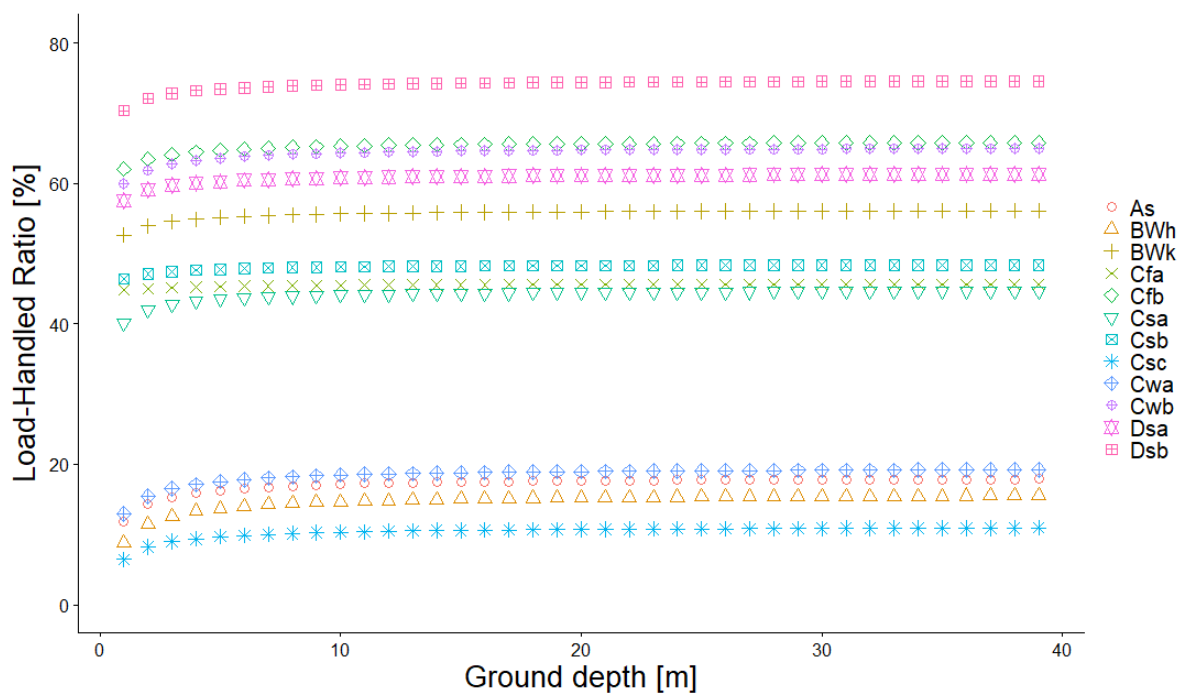


Figure 12. LHR of TABS depending on ground depth.

4. Conclusions

TABS integrated with horizontal ground exchanger was applied at different ground depths across 28 climates. LHR of TABS, considering freezing and condensation conditions, were evaluated to guide design engineers in selecting the appropriate ground depth depending on the weather conditions.

Analysis of the ground temperatures at different depths in various weather conditions shows that shallow ground temperature variations were similar to outdoor air temperature variations. In addition, in weather conditions with a high humidity ratio, the outdoor air temperature had less variation, resulting in only small changes in ground temperature. Thus, the amount of ground temperature variation in shallow depth could be assessed from the humidity ratio of the weather.

The depth of the ground temperature also significantly impacts ground temperature variations. Ground temperature variations become consistent in 2 m to 11 m depths depending on the outdoor air temperature variation. Since the typical depth of the horizontal ground system ranges from 0.5 m to 3, engineers should consider deeper depth depending on the weather conditions.

The risk of freezing the system fluid and surface condensation occurs in cold climates. The fluid in the system freezes for median outdoor air temperatures near freezing point temperature. However, an hourly evaluation should be conducted to decide the feasibility of the system. During the summer, the ground temperature in deep ground depth had a lower temperature, which increased the condensation risk.

A comparison of LHR with a typical TABS control strategy and TABS integrated with the horizontal ground system shows that the ground temperature is too high in hot weather conditions to provide free cooling. The maximum peak reduction reaches 75% with free cooling compared to the 32.4% achieved with the typical system with a chiller.

The LHR of TABS increased as the ground depth increased because the shallow ground temperature had a higher temperature during the peak period. The LHR varied up to 11% in a shallow depth, and after reaching a certain ground depth, LHR became consistent. The appropriate depth for maximizing the effectiveness of TABS for all cases is 8 m.

In future work, the effectiveness of the ground system with the application of heat recovery time will be conducted to increase the simulation accuracy. In addition, various

control strategies depending on the peak period and amount of cooling load will be studied to increase the LHR.

Author Contributions: W.J.C. produced the simulation results and drafted the manuscript. S.H.P. had an original idea and revised the manuscript. All authors have read and agreed to the published version of the manuscript.

Funding: This work was supported by the National Research Foundation of Korea (NRF) grant funded by the Korea government (MSIT) (No. NRF-2021R1F1A1046711).

Institutional Review Board Statement: Not applicable.

Informed Consent Statement: Not applicable.

Conflicts of Interest: The authors declare no conflict of interest.

References

1. Turner, W.J.N.; Walker, I.S.S.; Roux, J. Peak load reductions: Electric load shifting with mechanical pre-cooling of residential buildings with low thermal mass. *Energy* **2015**, *82*, 1057–1067. [\[CrossRef\]](#)
2. Reilly, A.; Kinnane, O. The impact of thermal mass on building energy consumption. *Appl. Energy* **2017**, *198*, 108–121. [\[CrossRef\]](#)
3. Elarga, H.; Fantucci, S.; Serra, V.; Zecchin, R.; Benini, E. Experimental and numerical analyses on thermal performance of different typologies of PCMs integrated in the roof space. *Energy Build.* **2017**, *150*, 546–557. [\[CrossRef\]](#)
4. Gao, Y.; Xu, J.; Yang, S.; Tang, X.; Zhou, Q.; Ge, J.; Xu, T.; Levinson, R. Cool roofs in China: Policy review, building simulations, and proof-of-concept experiments. *Energy Policy* **2014**, *74*, 190–214. [\[CrossRef\]](#)
5. Bevilacqua, P.; Bruno, R.; Arcuri, N. Green roofs in a Mediterranean climate: Energy performances based on in-situ experimental data. *Renew. Energy* **2020**, *152*, 1414–1430. [\[CrossRef\]](#)
6. Baeten, B.; Rogiers, F.; Helsen, L. Reduction of heat pump induced peak electricity use and required generation capacity through thermal energy storage and demand response. *Appl. Energy* **2017**, *195*, 184–195. [\[CrossRef\]](#)
7. Chung, W.J.; Lim, J.-H. Cooling operation guidelines of thermally activated building system considering the condensation risk in hot and humid climate. *Energy Build.* **2019**, *193*, 226–239. [\[CrossRef\]](#)
8. Babiak, J.; Olesen, B.W.; Petráš, D.; Olsen, B.W.; Petras, D.; Babiak, J.; Bjaren, W.; Olesen, D.P. *Low Temperature Heating and High Temperature Cooling*; REHVA: Brussels, Belgium, 2007; ISBN 2960046862.
9. Rijksen, D.O.O.; Wisse, C.J.J.; van Schijndel, A.W.M.W.M. Reducing peak requirements for cooling by using thermally activated building systems. *Energy Build.* **2010**, *42*, 298–304. [\[CrossRef\]](#)
10. Olesen, B.W.; Sommer, K.; Ducting, B. Control of slab heating and cooling systems studied by dynamic computer simulations. *ASHRAE Trans.* **2002**, *108*, 698.
11. Olesen, B.W. Thermo Active Building Systems: Using Building Mass To Heat and Cool. *ASHRAE J.* **2012**, *54*, 44–52.
12. Schmelas, M.; Feldmann, T.; Wellnitz, P.; Bollin, E. Adaptive predictive control of thermo-active building systems (TABS) based on a multiple regression algorithm: First practical test. *Energy Build.* **2016**, *129*, 367–377. [\[CrossRef\]](#)
13. Schmelas, M.; Feldmann, T.; Bollin, E. Adaptive predictive control of thermo-active building systems (TABS) based on a multiple regression algorithm. *Energy Build.* **2015**, *103*, 14–28. [\[CrossRef\]](#)
14. Arghand, T.; Javed, S.; Trüschel, A.; Dalenbäck, J.O. A comparative study on borehole heat exchanger size for direct ground coupled cooling systems using active chilled beams and TABS. *Energy Build.* **2021**, *240*, 110874. [\[CrossRef\]](#)
15. Huchtemann, K.; Müller, D. Combined simulation of a deep ground source heat exchanger and an office building. *Build. Environ.* **2014**, *73*, 97–105. [\[CrossRef\]](#)
16. Bockelmann, F.; Plessner, S.; Soldaty, H. *Rehva 20: Advanced System Design and Operation of GEOTABS Buildings*; REHVA: Brussels, Belgium, 2013; ISBN 9782930521121.
17. Lim, J.H.; Song, J.H.; Song, S.Y. Development of operational guidelines for thermally activated building system according to heating and cooling load characteristics. *Appl. Energy* **2014**, *126*, 123–135. [\[CrossRef\]](#)
18. Zhou, K.; Mao, J.; Li, Y.; Hua, Z. Comparative study on thermal performance of horizontal ground source heat pump systems with Dirichlet and Robin boundary conditions on ground surface. *Energy Convers. Manag.* **2020**, *225*, 113469. [\[CrossRef\]](#)
19. Cui, Y.; Zhu, J.; Twaha, S.; Chu, J.; Bai, H.; Huang, K.; Chen, X.; Zoras, S.; Soleimani, Z. Techno-economic assessment of the horizontal geothermal heat pump systems: A comprehensive review. *Energy Convers. Manag.* **2019**, *191*, 208–236. [\[CrossRef\]](#)
20. Geiger, R. Klassifikationen der Klimate nach W. Köppen. In *Landolf-Börnstein: Zahlenwerte und Funktionen aus Physik, Chemie, Astronomie, Geophysik und Technik, (Alte Serie)*; Springer: Berlin/Heidelberg, Germany, 1954; Volume 3, pp. 603–607.
21. Geiger, R. *Bearbeitete Neuausgabe von Geiger, R.: Köppen-Geiger/Klima der Erde. Wandkarte (Wall Map) 1: 16 Mill*; Klett-Perthes: Gotha, Germany, 1961.
22. Thornthwaite, C.W. *An Approach toward a Rational Classification of Climate*; American Geographical Society: New York, NY, USA, 1948; Volume 38.
23. Trewartha, G. *An Introduction to Climate*, 5th ed.; McGraw-Hill: New York, NY, USA, 1968.
24. Feddema, J.J. A Revised Thornthwaite-Type Global Climate Classification. *Phys. Geogr.* **2005**, *26*, 442–466. [\[CrossRef\]](#)

25. EnergyPlus Weather Data. Available online: <https://energyplus.net/weather> (accessed on 23 August 2021).
26. Kruis, N.; Krarti, M. KivaTM: A numerical framework for improving foundation heat transfer calculations. *J. Build. Perform. Simul.* **2015**, *8*, 449–468. [[CrossRef](#)]
27. Dinh, B.H.; Go, G.H.; Kim, Y.S. Performance of a horizontal heat exchanger for ground heat pump system: Effects of groundwater level drop with soil–water thermal characteristics. *Appl. Therm. Eng.* **2021**, *195*, 117203. [[CrossRef](#)]
28. Amadeh, A.; Habibi, M.; Hakkaki-Fard, A. Numerical simulation of a ground-coupled heat pump system with vertical plate heat exchangers: A comprehensive parametric study. *Geothermics* **2020**, *88*, 101913. [[CrossRef](#)]
29. Deru, M.; Field, K.; Studer, D.; Benne, K.; Griffith, B.; Torcellini, P.; Liu, B.; Halverson, M.; Winiarski, D.; Rosenberg, M.; et al. *U.S. Department of Energy Commercial Reference Building Models of the National Building Stock*; National Renewable Energy Laboratory: Golden, CO, USA, 2011.
30. Witte, M.J.; Henninger, R.H.; Glazer GARD Analytics, J.; Crawley, D.B. Testing and validation of a new building energy simulation program. In Proceedings of the Proceedings, Building Simulation, International Building Performance Simulation Association (IBSPA), Rio de Janeiro, Brazil, 13 August 2001; pp. 353–360.
31. Chantrasrisalai, C.; Ghatti, V.; Fisher, D.E.; Scheatzle, D.G. Experimental validation of the EnergyPlus low-temperature radiant simulation. *ASHRAE Trans.* **2003**, *109*, 614–623.
32. Witte, M.J.; Henninger, R.H.; Crawley, D.B. Experience testing EnergyPlus with the ASHRAE 1052-RP building fabric analytical tests. In Proceedings of the SimBuild 2004 IBPSA-USA National Conference, Boulder, CO, USA, 4–6 August 2004; pp. 1–8.
33. ASHRAE. *Standard 55: Thermal ENvironmental Conditions for Human Occupancy*; ASHRAE: Atlanta, GA, USA, 2013.
34. Park, S.H.; Chung, W.J.; Yeo, M.S.; Kim, K.W. Evaluation of the thermal performance of a Thermally Activated Building System (TABS) according to the thermal load in a residential building. *Energy Build.* **2014**, *73*, 69–82. [[CrossRef](#)]